nature chemistry

Article

https://doi.org/10.1038/s41557-023-01273-3

Selective scandium ion capture through coordination templating in a covalent organic framework

Received: 25 January 2021

Accepted: 9 June 2023

Published online: 03 July 2023

Check for updates

Ye Yuan[1,8], Yajie Yang[1,8], Katie R. Meihaus[2], Shenli Zhang[3], Xin Ge[4], Wei Zhang[4], Roland Faller[5], Jeffrey R. Long[2,6,7] & Guangshan Zhu[1]

The use of coordination complexes within covalent organic frameworks can significantly diversify the structures and properties of this class of materials. Here we combined coordination chemistry and reticular chemistry by preparing frameworks that consist of a ditopic (*p*-phenylenediamine) and mixed tritopic moieties—an organic ligand and a scandium coordination complex of similar sizes and geometries, both bearing terminal phenylamine groups. Changing the ratio of organic ligand to scandium complex enabled the preparation of a series of crystalline covalent organic frameworks with tunable levels of scandium incorporation. Removal of scandium from the material with the highest metal content subsequently resulted in a 'metal-imprinted' covalent organic framework that exhibits a high affinity and capacity for Sc^{3+} ions in acidic environments and in the presence of competing metal ions. In particular, the selectivity of this framework for Sc^{3+} over common impurity ions such as La^{3+} and Fe^{3+} surpasses that of existing scandium adsorbents.

Scandium is considered one of the rare earth metals, which—despite their name—are not especially uncommon; indeed, the abundance of scandium in the earth's crust is similar to that of cobalt and lithium. However, mineral deposits rich in scandium are few, and scandium is largely sourced as a by-product during the processing of iron, aluminium, lanthanides and other ores[1–4], where it is generally separated using solvent extraction after ore pretreating and leaching. Isolating scandium in useful quantities from parent ores is extremely costly—concentrations are as low as 10^{-4}% (ref. 5), and the energy required for the extraction and processing of scandium is estimated at ~97 GJ kg^{-1}, at least two orders of magnitude greater than for the lanthanides[6,7]. As a result, scandium is very expensive and used to a limited degree in industry, despite its recognition as a critical metal and demonstrated value in applications such as solid oxide fuel cells, lighting and high-performance alloys[8–10]. The development of new methods and materials for the selective, efficient and more sustainable extraction of scandium is therefore of great interest, and this area has been receiving increasing research attention in the past decade[8]. Recent efforts have led to the discovery of ionic liquids[11,12], functionalized silicas[13] and gels[14], among other materials[8], as candidates for scandium ion capture after the leaching of metal ores.

Porous adsorbents including metal–organic frameworks[15] and organic frameworks[16] have been investigated as versatile and robust adsorbents for the capture of various metal ions. Among these

[1]Key Laboratory of Polyoxometalate and Reticular Material Chemistry of Ministry of Education, Faculty of Chemistry, Northeast Normal University, Changchun, China. [2]Department of Chemistry, University of California, Berkeley, CA, USA. [3]Pritzker School of Molecular Engineering, University of Chicago, Chicago, IL, USA. [4]Key Laboratory of Automobile Materials MOE, and School of Materials Science & Engineering, and Electron Microscopy Center, and Jilin Provincial International Cooperation Key Laboratory of High-Efficiency Clean Energy Materials, Jilin University, Changchun, China. [5]Department of Chemical Engineering, University of California, Davis, CA, USA. [6]Department of Chemical & Biomolecular Engineering, University of California, Berkeley, CA, USA. [7]Materials Sciences Division, Lawrence Berkeley National Laboratory, Berkeley, CA, USA. [8]These authors contributed equally: Ye Yuan, Yajie Yang. e-mail: jrlong@berkeley.edu; Zhugs@nenu.edu.cn

materials, covalent organic frameworks (COFs)[17] have garnered particular interest, due to their low densities, high porosities and chemical diversity. For example, two- and three-dimensional COFs featuring carboxylate[18,19], thioether[20,21] and ethylenediaminetetraacetic acid functional groups[22] have been shown to capture mercury, cobalt and the lanthanides with a high selectivity. In these materials, the capture functionality is installed post-synthetically at one of the organic building units or introduced as part of a primary building unit prior to framework synthesis. The same synthetic approaches have also been used in the design of so-called metal–COFs, which have attracted interest for applications such as catalysis, conductivity and molecular separations because they combine the electronic diversity accessible in metal–organic frameworks with the robustness of a structure buttressed purely by covalent bonds[23]. These hybrid materials have predominantly been generated via post-synthetic metalation, with the exception of two-dimensional variants prepared with metalated porphyrin or phthalocyanine monomers[23,24].

Inspired by this emergent chemistry and the complementary concept of molecular imprinting in porous materials[25–27], we envisioned a different approach for the preparation of metal–COFs that uses metal coordination complexes as secondary building units. Such an approach should enable fine control over the extent of the metal site incorporation, while also providing coordination sites selective for a given metal. Herein we describe the design and synthesis of a family of COFs based on the parent material TpPa-1 (ref. 28) that feature varying quantities of Sc^{3+} coordination units (Fig. 1). The scandium ions can be released from these Sc–COFs to yield organic structures with 'imprinted' metal coordination sites that, to our knowledge, have not previously been accessed in another porous material. The imprinted framework with the highest density of coordination sites is highly selective for the uptake of Sc^{3+} over a number of other competing metal ions and is capable of extracting 98% of the scandium ions present in a nickel mineral sample with numerous competing metal ions at a pH of ~3. Notably, it is not necessary to use Sc^{3+} as the templating ion, and frameworks synthesized using secondary building units based on abundant divalent transition metal ions also yield metal-imprinted COFs (MICOFs) that are highly selective for scandium(III). The approach presented here affords a powerful means of designing diverse metal–covalent organic frameworks and imprinted COFs for selective metal ion capture.

Results and discussion

Synthesis and characterization of Sc–COFs and MICOFs

The robust, two-dimensional COF TpPa-1 served as our model structure for the design of a porous organic framework featuring Sc^{3+} binding pockets[28]. The structure is built of repeating keto-enamine salicylideneaniline units and forms following the irreversible tautomerization of the enol-imine precursor synthesized from 1,3,5-triformylphloroglucinol and *p*-phenylenediamine (Fig. 1a). We identified 4-aminophenylacetate as a suitable ligand for forming a trigonally symmetric, six-coordinate scandium complex that would be used as a secondary building unit for the hybrid COF (Fig. 1b)[29,30]. Based on energy minimization calculations, the proposed complex $Sc(C_8H_8NO_2)_3$ features Sc^{3+} in a distorted octahedral environment and has approximately the same size as the TpPa-1 repeat unit, with pendant amine groups suitable for the formation of an extended TpPa-1-type structure (Fig. 1c).

The complex was synthesized from the reaction of $ScCl_3{\cdot}6H_2O$ with 3 equiv. of 4-aminophenylacetic acid in a 4:1 (v/v) mixture of *N*,*N*′-dimethylformamide and water and isolated as a light yellow powder (Methods). The Fourier transform infrared (FT-IR) spectrum of the product features absorption bands at 1,540 and 1,455 cm^{-1} that are redshifted from the –C=O stretch of the free ligand (1,648 cm^{-1}) and were assigned to the asymmetric and symmetric –COO stretches of a scandium-bound carboxylate[29], respectively, while a new band at 508 cm^{-1} was assigned to a Sc–O vibration[29], supporting coordination of the carboxylate ligand to scandium (Supplementary Fig. 1). Proton and ^{13}C NMR spectra and mass spectrometry data also support complex formation (Supplementary Figs. 2 and 3). Further, X-ray photoelectron spectra collected for $Sc(C_8H_8NO_2)_3$ and the compound $Sc(O_2CC_{11}H_{23})_3$ ($O_2CC_{11}H_{23}^-$, laurate)[29] both feature a single Sc_{2p} peak at ~400 eV, confirming the presence of scandium(III) in similar coordination environments (Supplementary Fig. 4). Although the structure of $Sc(C_8H_8NO_2)_3$ has not been reported in the literature, analysis of FT-IR spectra obtained for that compound and several other scandium(III)–carboxylate complexes supports bidentate coordination. In particular, the difference between the asymmetric and symmetric –COO stretches for those compounds were found to be much smaller than the corresponding difference for a free carboxylate[29,30]. Similarly, here we found that this difference for our scandium complex (Δ = 85 cm^{-1}) is much smaller than that determined for $Na(C_2H_3O_2)$ (Δ = 140 cm^{-1})[31], which was used as a reference salt[29].

Scandium-loaded COFs were prepared via the solvothermal reaction of $Sc(C_8H_8NO_2)_3$ with 1,3,5-triformylphloroglucinol and *p*-phenylenediamine in a mixture of mesitylene, *N*,*N*-dimethylacetamide and aqueous acetic acid; a reaction time of 72 h was deemed optimal for obtaining crystalline material (Methods for further details). Precise molar ratios were used to prepare the parent TpPa-1 structure and metal–covalent organic frameworks with scandium occupying 9% to 43% of the parent structure 'nodes' (Fig. 1a), referred to as Sc–COF-9 through Sc–COF-43. The occurrence of a Schiff base reaction in all cases and incorporation of Sc^{3+} was verified by infrared, X-ray photoelectron and solid-state ^{13}C cross-polarization magic-angle-spinning NMR spectroscopies, as well as by elemental analysis (Supplementary Figs. 4–6 and Supplementary Table 2). Simulations performed in Materials Studio suggest that the substituted nodes in the Sc–COFs consist of one scandium ion coordinated by three 4-aminophenylacetate ligands, wherein the scandium centre adopts a distorted octahedral geometry with an average Sc–O bond length of 2.18 Å[30,32] and a C–CH_2–C angle of 128.5° (Fig. 1c).

In the Sc–COF infrared spectra, the characteristic –NH bands of *p*-phenylenediamine (3,200–3,500 cm^{-1}) are absent, while new bands associated with –C=C and –C–N vibrations are present at 1,578 and 1,255 cm^{-1} (Supplementary Fig. 5). All spectra additionally feature bands at 518 and 1,616 cm^{-1}, assigned to a Sc–O vibration and the –COO stretch of a scandium-bound carboxylate, respectively. X-ray photoelectron spectroscopy characterization of Sc–COF-33 revealed a Sc_{2p} peak with an energy of ~400 eV, identical to that of $Sc(C_8H_8NO_2)_3$ (Supplementary Fig. 4), confirming the presence of six-coordinate scandium(III) in the extended material. Finally, all peaks in the solid-state ^{13}C NMR spectrum of Sc–COF-33 could be assigned to the carbon atoms of the keto-enamine salicylideneaniline units or the scandium carboxylate ligands (Supplementary Fig. 6).

Powder X-ray diffraction data for Sc–COF-9 through Sc–COF-33 feature a series of broad peaks centred at 2θ = 4.7, 8.3, 12.6 and 27.0° (associated with the (100), (200), (210) and (001) crystal planes, respectively; 2θ, the angle between the transmitted beam and reflected beam), consistent with the diffraction pattern reported for the parent TpPa-1 structure[28] (Supplementary Fig. 7a). Accordingly, we propose that the Sc–COFs crystallize in the hexagonal space group *P*6/*m* with eclipsed stacking of the COF sheets[28], as previously established for TpPa-1. The π–π stacking distance between the layers in the Sc–COFs was determined to be ~3.4 Å, based on the *d*-spacing between the (001) planes[28]. We note that the diffraction peaks for the Sc–COF frameworks are quite broad, which may indicate the presence of an amorphous phase or simply a sample composed of very small crystallites[33]. Based on our electron microscopy data (given in the following sections), the crystallite size is on the order of a few nanometres, and thus we hypothesize that the broadening is due in large part to crystalline domain size.

Under identical experimental conditions, the characteristic diffraction peak of the (100) plane at 4.7° was chosen to evaluate the relative crystallinity of the Sc–COFs relative to a sample of TpPa-1.

https://doi.org/10.1038/s41557-023-01273-3

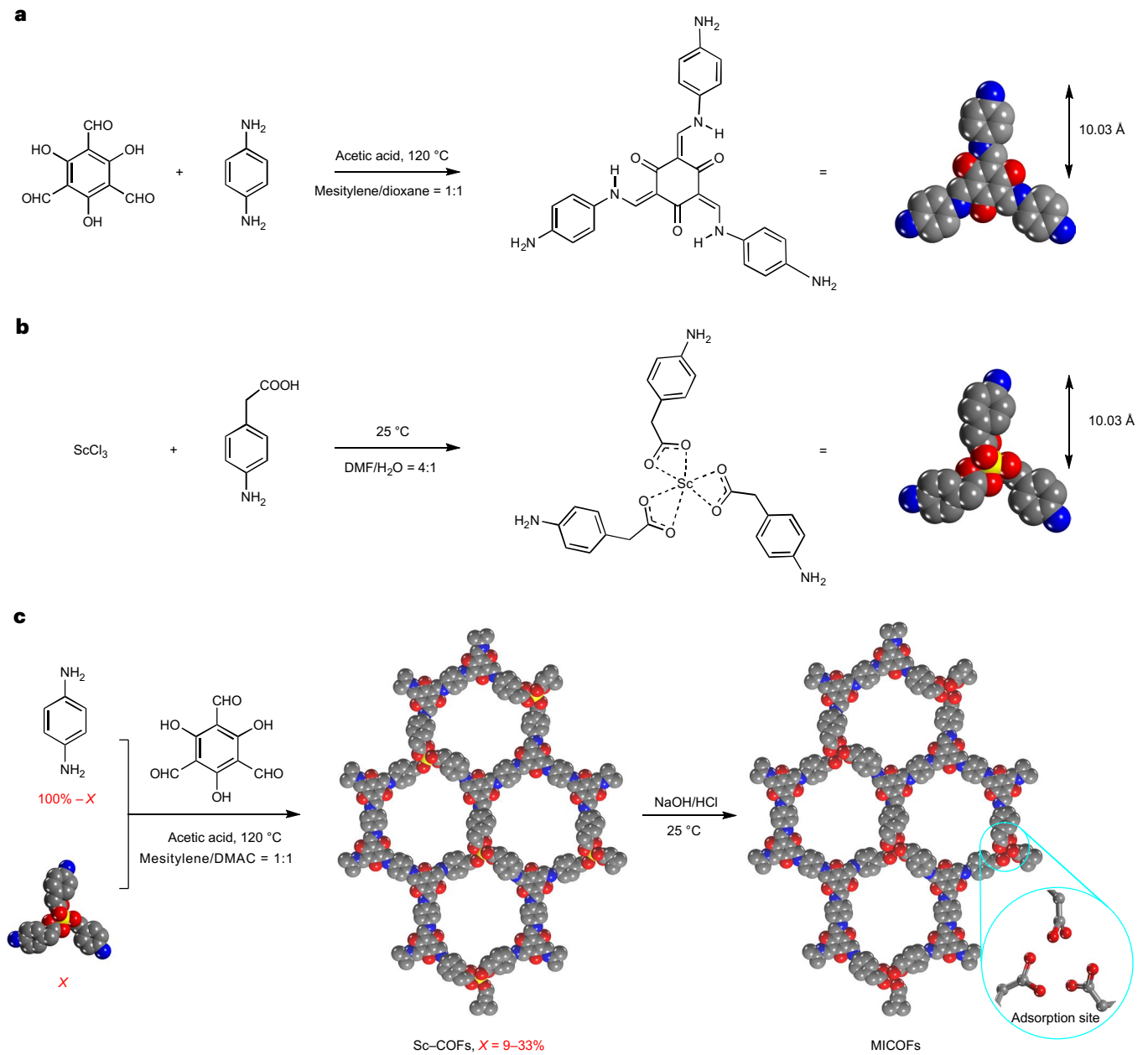

Fig. 1 | Design strategy and synthesis of the Sc–COFs and MICOFs. a, The parent COF structure chosen for this study, TpPa-1, is constructed from repeating keto-enamine salicylideneaniline units. **b**, To mimic the size, functionality and geometry of the TpPa-1 building units for the design of a hybrid Sc–COF, 4-aminophenylacetate was chosen as a ligand for the design of trigonal scandium complex secondary building units. DMF, *N*,*N*-dimethylformamide. **c**, Sc–COFs were prepared with varying degrees (X = 9, 17, 23, 29, 33%) of scandium ion incorporation. DMAC, *N*,*N*-dimethylacetamide. The Sc^{3+} ions can subsequently be removed to generate MICOFs with open coordination sites (enlarged view). All illustrations of the COF fragments/networks are models generated using Materials Studio. Scandium, oxygen, nitrogen and carbon atoms are represented as dark yellow, red, blue and grey spheres, respectively. Hydrogen atoms are omitted for clarity.

As the scandium complex content is increased from 0 to 33%, the relative intensity of the (100) peak decreases by only approximately 15%, while there is a clear peak shift and reduction in intensity when the scandium incorporation reaches 43%. The apparent structural degradation may be attributed in part to limited stability of the molecular scandium complex under the solvothermal conditions (Supplementary Fig. 9). However, it is also possible that the TpPa-1 structure is simply not stable to incorporation of scandium beyond ~33%, given that the inorganic building unit lacks the rigidity of the TpPa-1 repeating unit. Attempts to use tris(4-aminobenzoate) scandium(III) (without a methylene bridge), 4-aminophenylacetate in the absence of Sc^{3+}, or larger 1,3,5-tris(4-aminobiphenyl) benzene as secondary building units in the construction of TpPa-1-type structures resulted in only amorphous materials, highlighting the importance of the size, tailored flexibility and complex stability for framework synthesis (Supplementary Fig. 7).

Brunauer–Emmett–Teller surface areas of 676, 629, 581, 516, 479 and 436 $m^2\,g^{-1}$ were determined for TpPa-1, Sc–COF-9, Sc–COF-17, Sc–COF-23, Sc–COF-29 and Sc–COF-33, respectively, from N_2 adsorption data collected at 77 K (Fig. 2a and Supplementary Figs. 10 and 11). Framework pore size distribution was determined using non-local density functional theory[34], which revealed a peak at ~1.5 nm (Fig. 2b) in good agreement with the expected structure of TpPa-1.

https://doi.org/10.1038/s41557-023-01273-3

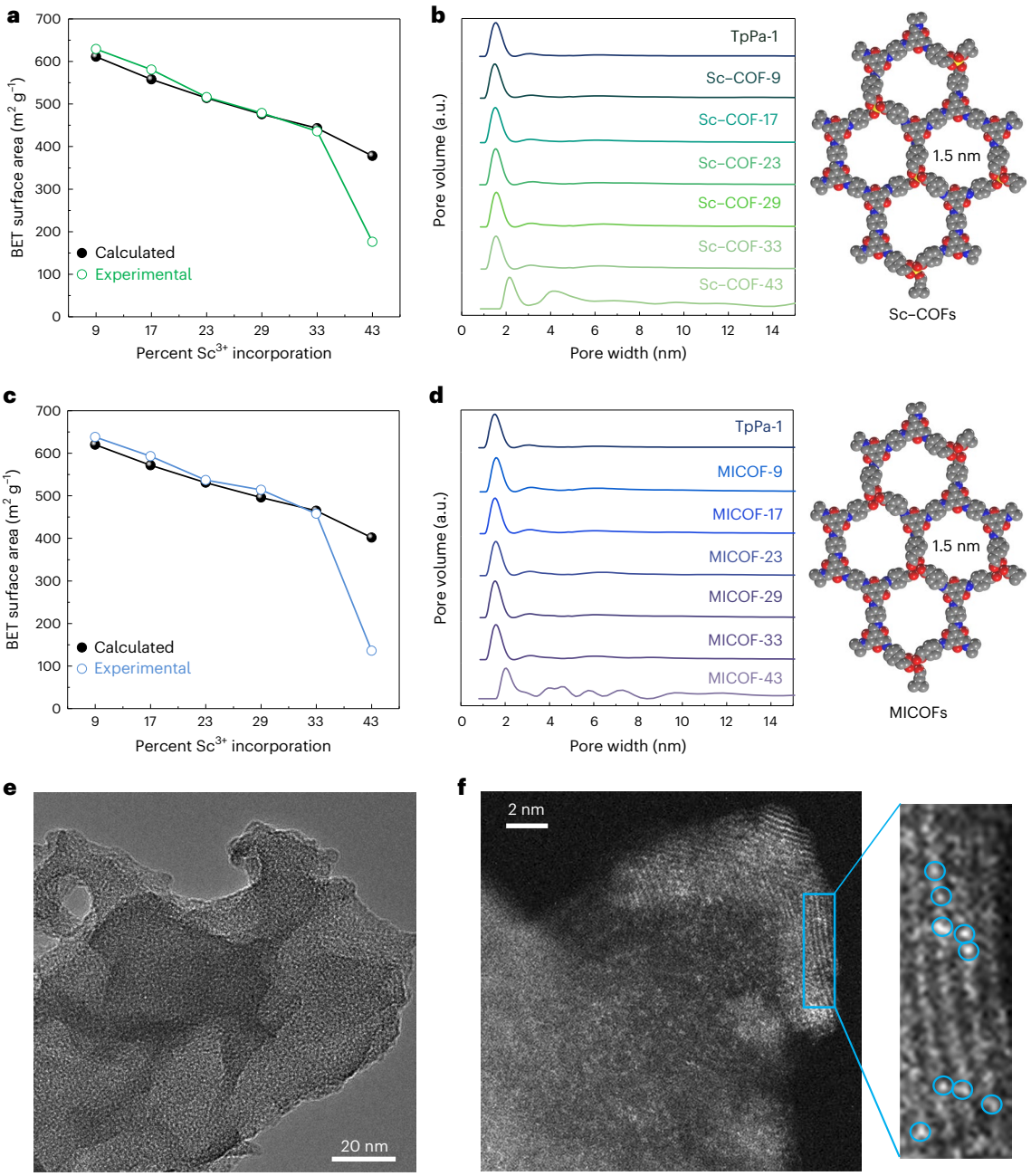

Fig. 2 | Characterization of Sc–COF-33. a–d, Experimental and theoretical Brunauer–Emmett–Teller (BET) surface areas (**a**,**c**) and pore size distributions (**b**,**d**) for the Sc–COFs (**a**,**b**) and MICOFs (**c**,**d**). The theoretical surface areas were determined starting from the Brunauer–Emmett–Teller surface area of TpPa-1 and calculating the change in mass and specific surface area upon replacing the COF structural unit with the varying quantities of the scandium(III) complex. On the right, illustrations of a portion of the Sc–COF (**b**) and MICOF (**d**) networks are shown as generated in Materials Studio. Scandium, oxygen, nitrogen and carbon atoms are represented as dark yellow, red, blue and grey spheres, respectively. Hydrogen atoms are omitted for clarity. **e**, TEM image of Sc–COF-33. **f**, High-angle annular dark-field STEM image of Sc–COF-33, where the scandium ions can be visualized as white dots; select scandium positions are highlighted with blue circles in the zoomed-in view.

Scanning electron microscopy characterization of Sc–COF-33 revealed aggregated particles with sizes ranging from 1 to 5 μm (Supplementary Fig. 12), while transmission electron microscopy (TEM) revealed a porous structure with a pore size of 1.5 nm (Fig. 2e), consistent with the results of the pore size distribution analysis. The presence of scandium was confirmed by using aberration-corrected scanning TEM (STEM; Fig. 2f and Supplementary Fig. 13). The high-angle annular dark-field STEM image of Sc–COF-33 features a multitude of bright dots corresponding to scandium ions that are well dispersed in the covalent matrix. The diameter of the dots is in the range of ~3 Å, suggesting that each bright dot corresponds to one individual Sc^{3+} ion. An expanded view of a portion of this image further suggests that each dot is embedded in the ordered framework structure and that there is no scandium cluster formation (Fig. 2f).

The Sc–COFs were treated with acid and base (Methods) to release the scandium ions[35] and generate framework materials featuring open coordination sites, referred to as MICOF-9 through MICOF-33. The Brunauer–Emmett–Teller surface areas of these materials are slightly greater than the parent COFs, as expected upon removal of the scandium ions, while the narrow pore size distributions (Fig. 2c,d) suggest

https://doi.org/10.1038/s41557-023-01273-3

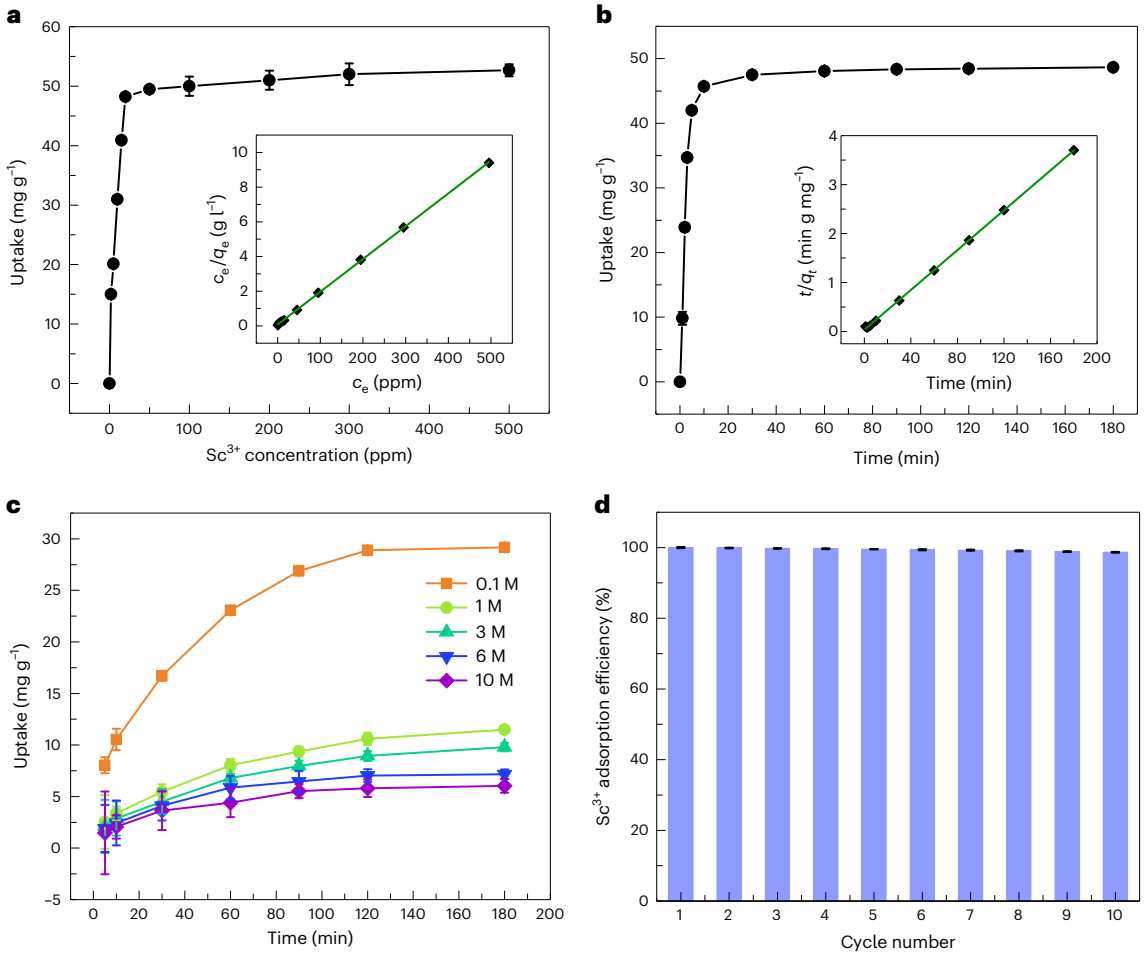

Fig. 3 | Scandium(III) uptake in MICOF-33. a, Scandium(III) adsorption isotherm collected for MICOF-33 at 298 K upon exposure to solutions of scandium(III) chloride hexahydrate dissolved in aqueous HCl (pH, ~5.5) with initial concentrations ranging from 2 to 500 ppm. The inset shows equilibrium adsorption data and a fit using a Langmuir model (R^2 = 0.9998; Supplementary Section 3.1 and Supplementary Table 3 for details), yielding a saturation capacity of 52.7 mg g^{-1}. R^2, correlation coefficient; C_e, ion concentration at equilibrium; q_e, ion sorption capacity at equilibrium. **b**, Scandium(III) uptake as a function of time (t) in MICOF-33 after exposure to a 20 ppm solution of aqueous scandium(III) chloride hexahydrate (pH, ~5.5). The inset show the fit of the time-dependent uptake data to a pseudo-second-order model (k_2 = 0.0124 g mg^{-1} min^{-1}, R^2 = 0.9997; Supplementary Section 3.2 and Supplementary Table 4). q_t, ion sorption capacity at time t. **c**, Time-dependent scandium(III) uptake in MICOF-33 as a function of HCl concentration. **d**, Cycling data for scandium(III) uptake in MICOF-33 from a 20 ppm aqueous solution (pH, ~5.5). Over the course of ten cycles, the capacity decreases by only 1.5%. Error bars in all panels represent the coefficient of variation obtained from three independent experiments.

that they retain crystallinity and the TpPa-1 structure. Indeed, the powder X-ray diffraction pattern of MICOF-33 is indistinguishable from that of Sc–COF-33 (Supplementary Fig. 14), indicating that π–π interactions between adjacent layers are sufficient to stabilize the structure upon removal of the scandium ions. Elemental analysis of MICOF-33 revealed that less than 0.1% scandium remains in the structure after acid/base treatment (Supplementary Table 2), and thermogravimetric analysis revealed that the MICOFs are stable up to 250 °C (Supplementary Fig. 16).

Scandium uptake in MICOF-33

Scandium(III) adsorption data were collected at 298 K for MICOF-33 exposed to concentrations ranging from 2 to 500 ppm (pH, ~5.5). The resulting adsorption isotherm (Fig. 3a) features an initial steep rise, indicating a strong affinity between the framework and Sc^{3+} ions, followed by a gradual plateau. At the highest examined Sc^{3+} concentration (500 ppm), the framework equilibrium capacity is 52.7 mg g^{-1}. The uptake data were fit with a Langmuir model (Fig. 3a, inset, and Supplementary Section 3.1), yielding a saturation capacity of 52.7 mg g^{-1}, which surpasses that of a number of reported scandium(III) adsorbents[14,36–38] (Supplementary Table 7). X-ray photoelectron spectroscopy characterization of MICOF-33 following scandium exposure revealed a Sc_{2p} peak with a binding energy identical to that of Sc–COF-33 and the scandium complex, confirming the successful uptake of Sc^{3+} at the vacant coordination sites (Supplementary Fig. 17). For the lowest initial Sc^{3+} concentration (2 ppm), 99.5% of the scandium was adsorbed after 48 h, corresponding to a large K_d of 1.01 × 10^6 ml g^{-1}. MICOF-33 also exhibits rapid Sc^{3+} adsorption kinetics, as seen in Fig. 3b. Rapid metal ion uptake occurs in the first 5 min before beginning to plateau at ~10 min, and the framework achieves 92% of its saturation capacity (48.6 mg g^{-1}) after 180 min.

Depending on source, composition and texture of a given mineral, many possible procedures may be required for extracting pure metals, including ore pretreating, leaching and solvent extraction[39]. Acidic leaching is a common process used to separate metal elements from mine tailings[39], and therefore it is highly desirable to realize an adsorbent capable of extracting scandium during the leaching stage. The uptake of Sc^{3+} in MICOF-33 and the framework stability were accordingly examined under varying concentrations of HCl (Fig. 3c). The capacity of Sc^{3+} decreases by less than 50% upon increasing the

https://doi.org/10.1038/s41557-023-01273-3

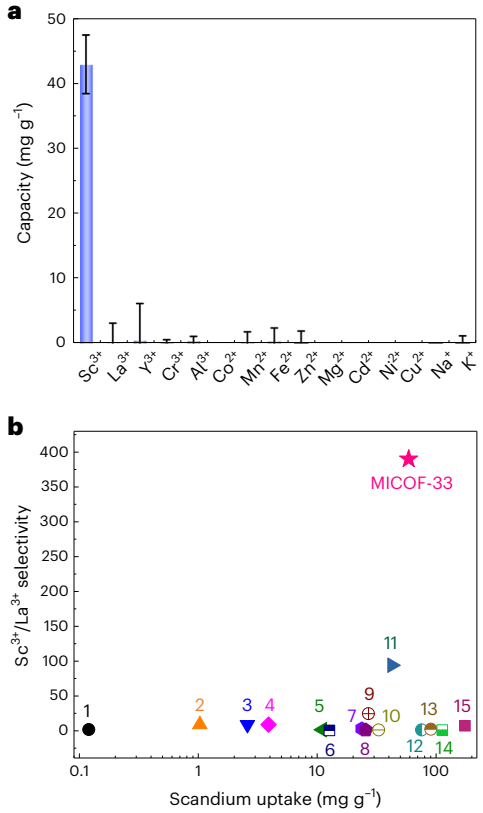

Fig. 4 | Scandium(III) uptake selectivity. a, Comparison of the equilibrium uptake of Sc^{3+} and various other metal ions in MICOF-33, highlighting the exceptional selectivity of the framework for scandium(III). **b**, Sc^{3+}/La^{3+} selectivity of MICOF-33 and reported adsorbents for scandium(III) capture. Supplementary Table 7 shows a full list of adsorbents by number, references and associated adsorption metrics. Error bars represent the standard deviation obtained from three independent experiments.

acid concentration by 30,000-fold, and even at the highest examined concentration of 10 M, the capacity remains moderate at 6.0 mg g^{-1}, exceeding the capacities of a number of scandium(III) adsorbents in the literature at higher pH values (Supplementary Table 7). Notably, MICOF-33 is also stable to repeated Sc^{3+} adsorption/desorption cycling at pH ~5.5 and exhibits a drop in capacity of only 0.7 mg g^{-1} (1.5%) after ten cycles (Fig. 3d).

Scandium ion selectivity

The selectivity of MICOF-33 for scandium(III) was examined by exposing a sample of the framework to an aqueous solution of HCl (pH, ~3) containing 20 ppm of the Sc^{3+} ion and 10 ppm of a number of competing metal ions (Na^{+}, K^{+}, Mg^{2+}, Mn^{2+}, Fe^{2+}, Cu^{2+}, Co^{2+}, Ni^{2+}, Zn^{2+}, Cd^{2+}, Al^{3+}, Cr^{3+}, Y^{3+} and La^{3+}; Supplementary Section 3.6). Importantly, the framework exhibits excellent selectivity for Sc^{3+} over all other examined metal ions (Fig. 4a), with selectivity coefficients (adsorbed mass ratios) ranging from 1.43×10^4 (Sc^{3+}/K^{+}) to 1.10×10^2 (Sc^{3+}/Fe^{2+}; Supplementary Table 6). The separation of iron(III) and scandium(III) is particularly challenging, given the similarity of their ionic radii and electronegativities[40], and MICOF-33 was also found to selectively capture Sc^{3+} over Fe^{3+} with a selectivity coefficient of 43. Of note, a control material with Tp (1,3,5-triformylphloroglucinol), Pa (p-phenylenediamine) and 33% 4-aminophenylacetic acid as building units adsorbed only 4.1 mg g^{-1} scandium(III) and exhibited far lower scandium selectivities ranging from 41.0 (Sc^{3+}/Na^{+}) to 1.20 (Sc^{3+}/Al^{3+}; Supplementary Fig. 18 and Supplementary Section 1.2 for details), highlighting the critical role of ion imprinting to generate an adsorbent selective for Sc^{3+}. To our knowledge, the selectivity of MICOF-33 for Sc^{3+} over the common impurity ions La^{3+} (Fig. 4b and Supplementary Table 7) and Fe^{3+} (Supplementary Table 8) surpasses that of Sc^{3+} adsorbents reported in the literature. Substantially, it is not necessary to use scandium(III) as the template ion in the formation of scandium-selective MICOF-33. Indeed, it was possible to synthesize the framework instead using Ni^{2+}, Mg^{2+} or Zn^{2+} complexes with 4-aminophenylacetate as secondary building units following the same synthetic protocol (Supplementary Section 7). MICOF-33 samples prepared in this way exhibit similar scandium(III) uptake to the MICOF-33 sample prepared using Sc^{3+} as a template and retain high selectivity for scandium over Ni^{2+}, Mg^{2+} or Zn^{2+}.

To elucidate the ultra-high selectivity of MICOF-33 for Sc^{3+}, density functional theory calculations were carried out to investigate the coordination environment of several different metal ions in neutral model complexes of the type $M(C_8H_7O_2)_3$ (Supplementary Section 5 for details). Calculations were implemented using Gaussian 16 code[41] with B3LYP/LANL2DZ+ empirical dispersion correction GD3 (ref. 42). The calculated $Sc(C_8H_7O_2)_3$ bond energy of 1.30×10^3 kJ mol^{-1} (representing the adsorption energy at one site in the MICOF structure) is larger than that determined for various transition metal ions, Mg^{2+} and Al^{3+} (0.51 to 1.17×10^3 kJ mol^{-1}; Supplementary Figs. 22 and 23 and Supplementary Table 10), and likewise the approximated stability constant for the model complex with Sc^{3+} is larger than for model compounds with the latter ions (Supplementary Section 5.1 and Supplementary Table 11), consistent with the selectivity of MICOF-33 for Sc^{3+} over these metal ions. Interestingly, the calculated bond energies for the Y^{3+} and La^{3+} complexes are competitive with that calculated for Sc^{3+} (and their estimated stability constants are larger), but uptake of these ions in MICOF-33 is far more sluggish: after 180 min, MICOF-33 achieves only 5.6% and 2.4% of its theoretical adsorption capacity for Y^{3+} and La^{3+}, respectively (Supplementary Table 12; compare with 91% in the case of Sc^{3+}). Time-dependent uptake data for Y^{3+} and La^{3+} were fit using a pseudo-second-order model (Supplementary Figs. 24 and 25) to yield k_2 values of 0.00134 and 0.00132 g mg^{-1} min^{-1}, respectively, which are approximately an order of magnitude lower than that determined for Sc^{3+} (0.0124 g mg^{-1} min^{-1}). Based on these data, it is likely that the larger ionic radii of these ions relative to the hydrated Sc^{3+} ion impede their facile access to the coordination cavities in the framework (also Supplementary Fig. 21). The results of our density functional theory calculations also serve to provide some rationale for the fact that samples of MICOF-33 prepared with different templating ions are still selective for scandium(III). In particular, in the calculated model compounds with Ni^{2+}, Zn^{2+} and Mg^{2+}, the ligand C–CH_2–C angles are 119.3°, 118.7° and 118.5°, respectively, whereas the corresponding angle for the Sc^{3+} compound was calculated to be 128.5°, which is much closer to the C–N–C angle of 127.5° in the optimized structure of the TpPa-1 molecular unit (Supplementary Figs. 19 and 20 and Supplementary Table 10). Thus, while molecular precursors with other metal cations may enable synthesis of the metal-loaded COF and MICOF-33, when competing metal ions are reintroduced, those most likely to be taken up are those that will lead to the most stable COF structure, in this case, Sc^{3+}.

Scandium extraction from minerals

A sample of nickel sulfide ore collected from Jilin, China, was acidified (pH, ~3) and treated with MICOF-33 to investigate the scandium(III) uptake properties of the framework from a real-world sample. After leaching, the initial metal ion solution was determined to contain Sc^{3+} (18.4 ppm), Al^{3+} (13.6 ppm), Fe^{3+} (4.8 ppm), Mg^{2+} (26.0 ppm), Ca^{2+} (888.4 ppm), Mn^{2+} (28.4 ppm), Co^{2+} (73.6 ppm), Ni^{2+} (14.0 ppm), Cu^{2+} (11.6 ppm), Zn^{2+} (6.8 ppm), Na^{+} (10,115.6 ppm) and K^{+} (116.4 ppm) by inductively coupled plasma mass spectrometry (ICP-MS). After 180 min, the MICOF-33 had adsorbed 98% of the Sc^{3+} present in the solution (corresponding to a capacity of 45.1 mg g^{-1}). Liberation of the captured scandium from the resulting sample using aqua regia yielded

a filtrate with a scandium(III) purity greater than 96%, as determined by ICP-MS (96.84% Sc^{3+}, 2.55% Fe^{3+}, 0.40% Al^{3+}, 0.21% Mn^{2+}). Notably, by carrying out five successive metal ion extraction and scrubbing operations using a 10 mg sample of MICOF-33 (Methods), it was possible to achieve a total of 423.7 µg of Sc^{3+} with a purity of 99.90%, suitable for applications in lighting and high-powered lasers[43,44]. From a preliminary sample calculation considering materials costs alone, based on these results, the cost to extract one kilogram of Sc^{3+} with 99.90% purity using MICOF-33 could be as low as approximately US$116 (Supplementary Table 9).

Conclusions

We have shown that the use of a specifically tailored Sc^{3+} coordination complex as a secondary building unit in the synthesis of the robust, two-dimensional framework TpPa-1 (ref. 28) yields stable metal–COFs that can be further treated to generate metal-imprinted frameworks selective for scandium ion capture. The material with the highest number of metal ion binding pockets, MICOF-33, exhibits excellent Sc^{3+} capacities, selectivities and cycling stability under acidic conditions, and it can be prepared from inexpensive, abundant transition metal ions, rendering it a promising candidate for practical use in scandium separation and purification from traditional mineral sources, as well as other scandium sources of interest such as electronics waste and bauxite residue[8]. More broadly, we envision the tunable synthetic approach presented here will serve as a powerful and generalizable route towards the synthesis of a class of hybrid metal–COFs and MICOFs tailored with coordination sites selective for different metal ions for diverse applications.

Online content

Any methods, additional references, Nature Portfolio reporting summaries, source data, extended data, supplementary information, acknowledgements, peer review information; details of author contributions and competing interests; and statements of data and code availability are available at https://doi.org/10.1038/s41557-023-01273-3.

References

1. Yasukawa, K. et al. A new and prospective resource for scandium: evidence from the geochemistry of deep-sea sediment in the western North Pacific Ocean. *Ore Geol. Rev.* **102**, 260–267 (2018).
2. Wang, W., Pranolo, Y. & Cheng, C. Y. Metallurgical processes for scandium recovery from various resources: a review. *Hydrometallurgy* **108**, 100–108 (2011).
3. Wang, W. & Cheng, C. Y. Separation and purification of scandium by solvent extraction and related technologies: a review. *J. Chem. Technol. Biot.* **86**, 1237–1246 (2011).
4. Chassé, M., Griffin, W. L., O'Reilly, S. Y. & Calas, G. Scandium speciation in a world-class lateritic deposit. *Geochem. Persp. Lett.* **3**, 105–114 (2017).
5. Zhang, P., You, S., Zhang, L., Feng, S. & Hou, S. A solvent extraction process for the preparation of ultrahigh purity scandium oxide. *Hydrometallurgy* **47**, 47–56 (1997).
6. Wilson, A. M. et al. Solvent extraction: the coordination chemistry behind extractive metallurgy. *Chem. Soc. Rev.* **43**, 123–134 (2014).
7. Li, J., Chen, C., Zhang, R. & Wang, X. Reductive immobilization of Re(VII) by graphene modified nanoscale zero-valent iron particles using a plasma technique. *Sci. China Chem.* **59**, 150–158 (2016).
8. Botelho Junior, A. B., Espinosa, D. C. R., Vaughan, J. & Tenório, J. A. S. Recovery of scandium from various sources: a critical review of the state of the art and future prospects. *Miner. Eng.* **172**, 107148 (2021).
9. Ahmad, Z. The properties and application of scandium-reinforced aluminum. *JOM* **55**, 35–39 (2003).
10. Das, S. et al. Extraction of scandium(III) from acidic solutions using organo-phosphoric acid reagents: a comparative study. *Sep. Purif. Technol.* **202**, 248–258 (2018).
11. Makanyire, T., Sanchez-Segado, S. & Jha, A. Separation and recovery of critical metal ions using ionic liquids. *Adv. Manuf.* **4**, 33–46 (2016).
12. Onghena, B. & Binnemans, K. Recovery of scandium(III) from aqueous solutions by solvent extraction with the functionalized ionic liquid betainium bis(trifluoromethylsulfonyl)imide. *Ind. Eng. Chem. Res.* **54**, 1887–1898 (2015).
13. Tu, Z. et al. Silica gel modified with 1-(2-aminoethyl)-3-phenylurea for selective solid-phase extraction and preconcentration of Sc(III) from environmental samples. *Talanta* **80**, 1205–1209 (2010).
14. Ramasamy, D. L., Puhakka, V., Doshi, B., Iftekhar, S. & Sillanpää, M. Fabrication of carbon nanotubes reinforced silica composites with improved rare earth elements adsorption performance. *Chem. Eng. J.* **365**, 291–304 (2019).
15. Peng, Y. et al. A versatile MOF-based trap for heavy metal ion capture and dispersion. *Nat. Commun.* **9**, 187 (2018).
16. Yuan, Y. & Zhu, G. Porous aromatic frameworks as a platform for multifunctional applications. *ACS Cent. Sci.* **5**, 409–418 (2019).
17. Diercks, C. S. & Yaghi, O. M. The atom, the molecule, and the covalent organic framework. *Science* **355**, eaal1585 (2017).
18. Yue, J.-Y. et al. Metal ion-assisted carboxyl-containing covalent organic frameworks for the efficient removal of Congo red. *Dalton Trans.* **48**, 17763–17769 (2019).
19. Lu, Q. et al. Postsynthetic functionalization of three-dimensional covalent organic frameworks for selective extraction of lanthanide ions. *Angew. Chem. Int. Ed.* **57**, 6042–6048 (2018).
20. Huang, N., Zhai, L., Xu, H. & Jiang, D. Stable covalent organic frameworks for exceptional mercury removal from aqueous solutions. *J. Am. Chem. Soc.* **139**, 2428–2434 (2017).
21. Sun, Q. et al. Postsynthetically modified covalent organic frameworks for efficient and effective mercury removal. *J. Am. Chem. Soc.* **139**, 2786–2793 (2017).
22. Jiang, Y., Liu, C. & Huang, A. EDTA-functionalized covalent organic framework for the removal of heavy-metal ions. *ACS Appl. Mater. Interfaces* **11**, 32186–32191 (2019).
23. Feng, X., Ding, X. & Jiang, D. Covalent organic frameworks. *Chem. Soc. Rev.* **41**, 6010–6022 (2012).
24. Dong, J., Han, X., Liu, Y., Li, H. & Cui, Y. Metal–covalent organic frameworks (MCOFs): a bridge between metal–organic frameworks and covalent organic frameworks. *Angew. Chem. Int. Ed.* **59**, 2–14 (2020).
25. Chen, L., Wang, X., Lu, W., Wu, X. & Li, J. Molecular imprinting: perspectives and applications. *Chem. Soc. Rev.* **45**, 2137–2211 (2016).
26. Yuan, Y., Yang, Y. & Zhu, G. Molecularly imprinted porous aromatic frameworks for molecular recognition. *ACS Cent. Sci.* **6**, 1082–1094 (2020).
27. Guo, Z. et al. Molecularly imprinted polymer/metal organic framework based chemical sensors. *Coatings* **6**, 42 (2016).
28. Kandambeth, S. et al. Construction of crystalline 2D covalent organic frameworks with remarkable chemical (acid/base) stability via a combined reversible and irreversible route. *J. Am. Chem. Soc.* **134**, 19524–19527 (2012).
29. Parashar, G. K. & Rai, A. K. Synthesis, molecular weights and infrared spectra of some scandium(III) higher carboxylates. *Transit. Met. Chem.* **3**, 49–50 (1978).
30. Rai, A. K. & Parashar, G. K. Synthesis and structural studies of some scandium(III) carboxylates. *Synth. React. Inorg. Met. Org. Chem.* **9**, 301–307 (1979).
31. Zhang, X., Kumar, R. & Kuroda, D. G. Acetate ion and its interesting solvation shell structure and dynamics. *J. Chem. Phys.* **148**, 094506 (2018).

32. Anderson, T., Neuman, M. & Melson, G. Coordination chemistry of scandium. VI. Crystal and molecular structure of tris(tropolonato) scandium(III). Stereochemistry of some six-coordinate complexes. *Inorg. Chem.* **13**, 158–163 (1974).
33. Holder, C. F. & Schaak, R. E. Tutorial on powder X-ray diffraction for characterizing nanoscale materials. *ACS Nano* **13**, 7359–7365 (2019).
34. Ravikovitcha, P. I., Haller, G. L. & Neimark, A. V. Density functional theory model for calculating pore size distributions: pore structure of nanoporous catalysts. *Adv. Colloid Interface Sci.* **76–77**, 203–226 (1998).
35. Jiang, J., Zhao, Y. & Yaghi, O. M. Covalent chemistry beyond molecules. *J. Am. Chem. Soc.* **138**, 3255–3265 (2016).
36. Zhang, N., Huang, C. & Hu, B. ICP-AES determination of trace rare earth elements in environmental and food samples by on-line separation and preconcentration with acetylacetone-modified silica gel using microcolumn. *Anal. Sci.* **23**, 997–1002 (2007).
37. Iftekhar, S., Srivastava, V. & Sillanpää, M. Enrichment of lanthanides in aqueous system by cellulose based silica nanocomposite. *Chem. Eng. J.* **320**, 151–159 (2017).
38. Ramasamy, D., Puhakka, V., Repo, E., Khan, S. & Sillanpää, M. Coordination and silica surface chemistry of lanthanides (III), scandium (III) and yttrium (III) sorption on 1-(2-pyridylazo)-2-napththol (PAN) and acetylacetone (acac) immobilized gels. *Chem. Eng. J.* **324**, 104–112 (2017).
39. Wang, W., Pranolo, Y. & Cheng, C. Y. Metallurgical processes for scandium recovery from various resources: a review. *Hydrometallurgy* **108**, 100–108 (2011).
40. Shannon, R. D. Revised effective ionic radii and systematic studies of interatomic distances in halides and chalcogenides. *Acta Cryst.* **A32**, 751–767 (1976).
41. Frisch, M. J. et al. Gaussian 16, Revision C (Gaussian, 2016).
42. Wei, D. et al. Adsorption properties of hydrated Cr^{3+} ions on Schiff-base covalent organic frameworks: a DFT study. *Chem. Asian J.* **15**, 1140–1146 (2020).
43. Spedding, F. H. & Croat, J. J. Magnetic properties of high purity scandium and the effect of impurities on these properties. *J. Chem. Phys.* **58**, 5514–5526 (1973).
44. Bunzli, J.-C. G. & Choppin, G. R. (eds) *Lanthanide Probes in Life, Chemical and Earth Sciences* (Elsevier, 1989).

Methods

Preparation of scandium(III) complex, $Sc(C_8H_8NO_2)_3$

$ScCl_3{\cdot}6H_2O$ (259.4 mg, 1.000 mmol) and 4-aminophenylacetic acid (453.5 mg, 3.000 mmol) were dissolved in a 5 ml DMF and water mixture (v/v, 4:1) and stirred for 3 h at room temperature. After removal of the solvent under vacuum, 10 ml DMF was added to Sc-complex powder (500 mg), the mixture was sonicated for 30 min and the resulting solid was collected by filtration. The solid was then added to 10 ml H_2O, the mixture was sonicated for 30 min and the solid was again isolated by filtration. The latter steps were repeated two times and the solid was collected by filtration and finally dried under vacuum at 50 °C for 12 h to yield $Sc(C_8H_8NO_2)_3$ (442.4 mg, 89.3%). ^{1}H NMR (500 MHz, dimethyl sulfoxide (DMSO)) δ 6.89 (*d*, J = 8.3 Hz, ^{2}H), 6.50 (*d*, J = 8.3 Hz, ^{2}H), 5.01 (*s*, ^{2}H), 3.33 (*s*, ^{2}H). ^{13}C NMR (126 MHz, DMSO) δ 175.98, 147.27, 130.14, 123.47, 114.44, 41.02 ppm. Infrared results are as follows: 3,370, 2,862, 2,580, 1,984, 1,540, 1,512, 1,455, 1,422, 1,414, 1,386, 1,331, 1,306, 1,282, 1,209, 1,179, 1,168, 1,119, 1,021, 961, 929, 862, 812, 796, 723, 691, 616, 577, 508, 499, 421 cm^{-1}. High-resolution mass spectrometry (*m*/*z*) results are as follows: $[M + H]^+$ calculated for $C_{24}H_{25}N_3O_6Sc$, 496.43; found, 496.2981. Elemental analysis calculated results (%) are C, 58.18; H, 4.88; N, 8.48; Sc, 9.07; found (%) are C, 58.09; H, 5.08; N, 8.36; Sc, 8.93 (average of three samples).

Preparation of Sc–COFs

Triformylphloroglucinol (25.2 mg, 0.120 mmol) was combined with *p*-phenylenediamine and $Sc(C_8H_8NO_2)_3$ in varying molar ratios to yield Sc–COF-9 (0.162 and 0.0120 mmol, respectively), Sc–COF-17 (0.144 and 0.0240 mmol, respectively), Sc–COF-23 (0.126 and 0.0360 mmol, respectively), Sc–COF-29 (0.108 and 0.0480 mmol, respectively) and Sc–COF-33 (0.0900 and 0.0600 mmol, respectively). In each case, the reagents were combined together in a Pyrex tube with mesitylene (0.6 ml), *N*,*N*-dimethylacetamide (0.6 ml) and acetic acid (0.2 ml, 3 M). Each Pyrex tube was sonicated to homogenize the mixture, flash frozen at 77 K and degassed over three freeze–pump–thaw cycles. Finally, the Pyrex tubes were sealed and heated at 120 °C for 72 h. The tubes were then cooled to room temperature, and the resulting solids were filtered, washed three times with *N*,*N*-dimethylacetamide and acetone and then dried under vacuum at 100 °C to obtain the Sc–COFs (43.2 mg, 74.3%). Solid-state ^{13}C magic-angle-spinning NMR (101 MHz) δ 183.11, 173.72, 146.74, 134.83, 120.22, 114.24, 105.95, 39.95. Infrared results are as follows: 1,724, 1,616, 1,578, 1,516, 1,452, 1,289, 1,255, 1,092, 993, 826, 610, 554, 518 cm^{-1}. Note that reaction times longer than 72 h did not obviously enhance the material crystallinity (Supplementary Fig. 8 and Supplementary Table 1). Elemental analysis results for the Sc–COF samples are given in Supplementary Table 2.

Preparation of MICOFs

Some 1 M NaOH (10 ml) was added to each of the Sc–COF samples (10.0 mg), the mixtures were sonicated for 30 min and the resulting solids were collected by filtration. The solids were then added to 1 M aqueous HCl (10 ml), the mixtures were sonicated for 30 min and the solids were again isolated by filtration. The latter steps were repeated two times and the solids were collected by filtration and washed by distilled water (10 ml) and acetone (10 ml). The solids were finally dried under vacuum at 100 °C for 12 h, yielding the MICOF samples (39.8 mg, 96.5%). Solid-state ^{13}C magic-angle-spinning NMR (101 MHz) δ 183.91, 172.99, 147.36, 135.73, 119.54, 115.28, 107.07, 40.33. Infrared results are as follows: 1,572, 1,558, 1,539, 1,518, 1,509, 1,487, 1,472, 1,450, 1,419, 1,251, 1,231, 1,152, 1,076, 1,053, 993, 944, 807, 702, 640, 608, 552, 518, 430, 419, 409 cm^{-1}. Elemental analysis results for the MICOF samples are given in Supplementary Table 2.

Purification of scandium(III) from nickel ore

A treated sample of nickel ore from Jilin, China, was dissolved in 100 ml of aqueous HCl (pH, ~3) and determined by ICP-MS to contain the following metal ions: Sc^{3+} (18.4 ppm), Al^{3+} (13.6 ppm), Fe^{3+} (4.8 ppm), Mg^{2+} (26.0 ppm), Ca^{2+} (888.4 ppm), Mn^{2+} (28.4 ppm), Co^{2+} (73.6 ppm), Ni^{2+} (14.0 ppm), Cu^{2+} (11.6 ppm), Zn^{2+} (6.8 ppm), Na^+ (10,115.6 ppm) and K^+ (116.4 ppm). A 40 mg sample of MICOF-33 was added to this solution, and the mixture was stirred for 180 min. The framework solid was then collected by filtration and dried under vacuum at 100 °C. The metalated framework sample was then treated with 1 M NaOH (10 ml), and the mixture was sonicated for 30 min. The resulting solids were collected by filtration, and the filtrate was set aside. The solids were then added to 1 M aqueous HCl (10 ml), the mixtures were sonicated for 30 min and the solids were again isolated by filtration, and the filtrate set aside. The latter steps were repeated two times, the solids were collected by filtration and the scandium(III)-rich filtrates were combined. The isolated solid was washed by distilled water (10 ml) and acetone (10 ml) and finally dried under vacuum at 100 °C for 12 h, yielding the regenerated MICOF-33 sample. The filtrate was acidified to a pH of ~3, and the regenerated MICOF-33 sample was added to this solution and stirred for 180 min. Five additional adsorption/regeneration cycles were carried out in this manner to yield a scandium filtrate containing 99.90% pure Sc^{3+} ion, as determined by ICP-MS.

Reporting summary

Further information on research design is available in the Nature Portfolio Reporting Summary linked to this article.

Data availability

The authors declare that the main data supporting the findings of this study can be accessed at https://doi.org/10.6084/m9.figshare.19602262 (ref. 45). Source data are provided with this paper.

References

45. Yaun, Y. Data for selective scandium ion capture through coordination templating in a covalent organic framework. *figshare* https://figshare.com/s/307112ae4822adc40e38 (2023).

Acknowledgements

G.Z. was supported by the National Key R&D Program of China (grant no. 2022YFB3805902), the National Natural Science Foundation of China (grant nos 22131004 and U21A20330) and the '111' project (grant no. B18012). Y. Yang was supported by the National Natural Science Foundation of China (grant no. 52204389). Y. Yuan was supported by the National Natural Science Foundation of China (grant no. 21975039) and the Fundamental Research Funds for the Central Universities, Excellent Youth Team Program (grant no. 2412023YQ001). K.R.M. and J.R.L. were supported by the US Department of Energy, Office of Science, Office of Basic Energy Sciences under award DE-SC0019992.

Author contributions

Y. Yang carried out the experiments, performed the data interpretation and draughted the initial manuscript. X.G. and W.Z. collected and analysed the TEM and STEM data. J.R.L. and K.R.M. helped design the experiments and wrote portions of the manuscript. S.Z. and R.F. performed the theoretical calculations. Y. Yuan and G.Z. developed the concept, supervised the experiments and draughted the manuscript.

Competing interests

The authors declare no competing interests.

Additional information

Supplementary information The online version contains supplementary material available at https://doi.org/10.1038/s41557-023-01273-3.

Correspondence and requests for materials should be addressed to Jeffrey R. Long or Guangshan Zhu.

Peer review information *Nature Chemistry* thanks Shengqian Ma, Dan Zhao and the other, anonymous, reviewer(s) for their contribution to the peer review of this work.

nature portfolio

Corresponding author(s): Guangshan Zhu

Last updated by author(s): Sep 15, 2022

Reporting Summary

Nature Portfolio wishes to improve the reproducibility of the work that we publish. This form provides structure for consistency and transparency in reporting. For further information on Nature Portfolio policies, see our Editorial Policies and the Editorial Policy Checklist.

Statistics

For all statistical analyses, confirm that the following items are present in the figure legend, table legend, main text, or Methods section.

n/a	Confirmed	
☐	☒	The exact sample size (*n*) for each experimental group/condition, given as a discrete number and unit of measurement
☐	☒	A statement on whether measurements were taken from distinct samples or whether the same sample was measured repeatedly
☐	☒	The statistical test(s) used AND whether they are one- or two-sided *Only common tests should be described solely by name; describe more complex techniques in the Methods section.*
☐	☒	A description of all covariates tested
☐	☒	A description of any assumptions or corrections, such as tests of normality and adjustment for multiple comparisons
☐	☒	A full description of the statistical parameters including central tendency (e.g. means) or other basic estimates (e.g. regression coefficient) AND variation (e.g. standard deviation) or associated estimates of uncertainty (e.g. confidence intervals)
☐	☒	For null hypothesis testing, the test statistic (e.g. *F*, *t*, *r*) with confidence intervals, effect sizes, degrees of freedom and *P* value noted *Give P values as exact values whenever suitable.*
☐	☒	For Bayesian analysis, information on the choice of priors and Markov chain Monte Carlo settings
☐	☒	For hierarchical and complex designs, identification of the appropriate level for tests and full reporting of outcomes
☐	☒	Estimates of effect sizes (e.g. Cohen's *d*, Pearson's *r*), indicating how they were calculated

Our web collection on statistics for biologists contains articles on many of the points above.

Software and code

Policy information about availability of computer code

Data collection	No software was used.
Data analysis	Chemdraw Professional 16.0, Origin 2017, Adobe Photoshop CS64.

For manuscripts utilizing custom algorithms or software that are central to the research but not yet described in published literature, software must be made available to editors and reviewers. We strongly encourage code deposition in a community repository (e.g. GitHub). See the Nature Portfolio guidelines for submitting code & software for further information.

Data

Policy information about availability of data

All manuscripts must include a data availability statement. This statement should provide the following information, where applicable:

- Accession codes, unique identifiers, or web links for publicly available datasets
- A description of any restrictions on data availability
- For clinical datasets or third party data, please ensure that the statement adheres to our policy

The datasets generated during and/or analysed during the current study are available from the corresponding author on reasonable request.

Human research participants

Policy information about studies involving human research participants and Sex and Gender in Research.

Reporting on sex and gender	*Use the terms sex (biological attribute) and gender (shaped by social and cultural circumstances) carefully in order to avoid confusing both terms. Indicate if findings apply to only one sex or gender; describe whether sex and gender were considered in study design whether sex and/or gender was determined based on self-reporting or assigned and methods used. Provide in the source data disaggregated sex and gender data where this information has been collected, and consent has been obtained for sharing of individual-level data; provide overall numbers in this Reporting Summary. Please state if this information has not been collected. Report sex- and gender-based analyses where performed, justify reasons for lack of sex- and gender-based analysis.*
Population characteristics	*Describe the covariate-relevant population characteristics of the human research participants (e.g. age, genotypic information, past and current diagnosis and treatment categories). If you filled out the behavioural & social sciences study design questions and have nothing to add here, write "See above."*
Recruitment	*Describe how participants were recruited. Outline any potential self-selection bias or other biases that may be present and how these are likely to impact results.*
Ethics oversight	*Identify the organization(s) that approved the study protocol.*

Note that full information on the approval of the study protocol must also be provided in the manuscript.

Field-specific reporting

Please select the one below that is the best fit for your research. If you are not sure, read the appropriate sections before making your selection.

☐ Life sciences ☐ Behavioural & social sciences ☐ Ecological, evolutionary & environmental sciences

For a reference copy of the document with all sections, see nature.com/documents/nr-reporting-summary-flat.pdf

Life sciences study design

All studies must disclose on these points even when the disclosure is negative.

Sample size	*Describe how sample size was determined, detailing any statistical methods used to predetermine sample size OR if no sample-size calculation was performed, describe how sample sizes were chosen and provide a rationale for why these sample sizes are sufficient.*
Data exclusions	*Describe any data exclusions. If no data were excluded from the analyses, state so OR if data were excluded, describe the exclusions and the rationale behind them, indicating whether exclusion criteria were pre-established.*
Replication	*Describe the measures taken to verify the reproducibility of the experimental findings. If all attempts at replication were successful, confirm this OR if there are any findings that were not replicated or cannot be reproduced, note this and describe why.*
Randomization	*Describe how samples/organisms/participants were allocated into experimental groups. If allocation was not random, describe how covariates were controlled OR if this is not relevant to your study, explain why.*
Blinding	*Describe whether the investigators were blinded to group allocation during data collection and/or analysis. If blinding was not possible, describe why OR explain why blinding was not relevant to your study.*

Behavioural & social sciences study design

All studies must disclose on these points even when the disclosure is negative.

Study description	*Briefly describe the study type including whether data are quantitative, qualitative, or mixed-methods (e.g. qualitative cross-sectional, quantitative experimental, mixed-methods case study).*
Research sample	*State the research sample (e.g. Harvard university undergraduates, villagers in rural India) and provide relevant demographic information (e.g. age, sex) and indicate whether the sample is representative. Provide a rationale for the study sample chosen. For studies involving existing datasets, please describe the dataset and source.*
Sampling strategy	*Describe the sampling procedure (e.g. random, snowball, stratified, convenience). Describe the statistical methods that were used to predetermine sample size OR if no sample-size calculation was performed, describe how sample sizes were chosen and provide a rationale for why these sample sizes are sufficient. For qualitative data, please indicate whether data saturation was considered, and what criteria were used to decide that no further sampling was needed.*

Data collection	*Provide details about the data collection procedure, including the instruments or devices used to record the data (e.g. pen and paper, computer, eye tracker, video or audio equipment) whether anyone was present besides the participant(s) and the researcher, and whether the researcher was blind to experimental condition and/or the study hypothesis during data collection.*
Timing	*Indicate the start and stop dates of data collection. If there is a gap between collection periods, state the dates for each sample cohort.*
Data exclusions	*If no data were excluded from the analyses, state so OR if data were excluded, provide the exact number of exclusions and the rationale behind them, indicating whether exclusion criteria were pre-established.*
Non-participation	*State how many participants dropped out/declined participation and the reason(s) given OR provide response rate OR state that no participants dropped out/declined participation.*
Randomization	*If participants were not allocated into experimental groups, state so OR describe how participants were allocated to groups, and if allocation was not random, describe how covariates were controlled.*

Ecological, evolutionary & environmental sciences study design

All studies must disclose on these points even when the disclosure is negative.

Study description	*Briefly describe the study. For quantitative data include treatment factors and interactions, design structure (e.g. factorial, nested, hierarchical), nature and number of experimental units and replicates.*
Research sample	*Describe the research sample (e.g. a group of tagged Passer domesticus, all Stenocereus thurberi within Organ Pipe Cactus National Monument), and provide a rationale for the sample choice. When relevant, describe the organism taxa, source, sex, age range and any manipulations. State what population the sample is meant to represent when applicable. For studies involving existing datasets, describe the data and its source.*
Sampling strategy	*Note the sampling procedure. Describe the statistical methods that were used to predetermine sample size OR if no sample-size calculation was performed, describe how sample sizes were chosen and provide a rationale for why these sample sizes are sufficient.*
Data collection	*Describe the data collection procedure, including who recorded the data and how.*
Timing and spatial scale	*Indicate the start and stop dates of data collection, noting the frequency and periodicity of sampling and providing a rationale for these choices. If there is a gap between collection periods, state the dates for each sample cohort. Specify the spatial scale from which the data are taken*
Data exclusions	*If no data were excluded from the analyses, state so OR if data were excluded, describe the exclusions and the rationale behind them, indicating whether exclusion criteria were pre-established.*
Reproducibility	*Describe the measures taken to verify the reproducibility of experimental findings. For each experiment, note whether any attempts to repeat the experiment failed OR state that all attempts to repeat the experiment were successful.*
Randomization	*Describe how samples/organisms/participants were allocated into groups. If allocation was not random, describe how covariates were controlled. If this is not relevant to your study, explain why.*
Blinding	*Describe the extent of blinding used during data acquisition and analysis. If blinding was not possible, describe why OR explain why blinding was not relevant to your study.*

Did the study involve field work? ☐ Yes ☐ No

Field work, collection and transport

Field conditions	*Describe the study conditions for field work, providing relevant parameters (e.g. temperature, rainfall).*
Location	*State the location of the sampling or experiment, providing relevant parameters (e.g. latitude and longitude, elevation, water depth).*
Access & import/export	*Describe the efforts you have made to access habitats and to collect and import/export your samples in a responsible manner and in compliance with local, national and international laws, noting any permits that were obtained (give the name of the issuing authority, the date of issue, and any identifying information).*
Disturbance	*Describe any disturbance caused by the study and how it was minimized.*

Reporting for specific materials, systems and methods

We require information from authors about some types of materials, experimental systems and methods used in many studies. Here, indicate whether each material, system or method listed is relevant to your study. If you are not sure if a list item applies to your research, read the appropriate section before selecting a response.

Materials & experimental systems

n/a	Involved in the study
☒	☐ Antibodies
☒	☐ Eukaryotic cell lines
☒	☐ Palaeontology and archaeology
☒	☐ Animals and other organisms
☒	☐ Clinical data
☒	☐ Dual use research of concern

Methods

n/a	Involved in the study
☒	☐ ChIP-seq
☒	☐ Flow cytometry
☒	☐ MRI-based neuroimaging